

## Photoluminescence and Optical Absorption of Pure Nanocrystalline TiO<sub>2</sub> Anatase and Rutile at Room Temperature

L. Kernazhitsky<sup>1,\*</sup>, V. Shymanovska<sup>1</sup>, T. Gavrilko<sup>1</sup>, V. Naumov<sup>2</sup>, L. Fedorenko<sup>2</sup>, V. Kshnyakin<sup>3</sup>

<sup>1</sup> Institute of Physics, NAS of Ukraine, 46, Pr. Nauky, 03650 Kyiv, Ukraine

<sup>2</sup> Institute of Semiconductor V.E. Lashkareva, NAS of Ukraine, 41, Pr. Nauki, 03028 Kyiv, Ukraine

<sup>3</sup> Sumy State University, 2, Rimsky-Korsakov Str., 40007 Sumy, Ukraine

(Received 12 April 2013; published online 17 October 2013)

The optical absorption and photoluminescence of nanocrystalline TiO<sub>2</sub> samples of anatase and rutile were investigated at room temperature. Nanocrystalline TiO<sub>2</sub> samples were synthesized in the form of pure anatase or rutile and studied by X-ray diffraction, X-ray fluorescence, Raman spectroscopy, optical absorption and photoluminescence (PL). PL was studied at room temperature when excited by intense UV (3.68 eV) by a nitrogen laser. For the first time for nanocrystalline TiO<sub>2</sub> features in the high-resolution PL spectra including the exciton band and interband transitions were registered. It is concluded that the processes of absorption and emission of light near the edge of the forbidden zone occur with the participation of the same electronic transitions. PL bands, including the peaks at 2.71-2.81 eV in the anatase and rutile arise due to exciton recombination in the TiO<sub>2</sub> lattice oxygen vacancies. The exciton peak at 2.91 eV is attributed to the recombination of self-trapped excitons in anatase or to the free exciton in rutile, respectively. PL bands within 3.0-3.3 eV attributed to indirect and direct allowed transitions due to electron-hole recombination. PL bands at 3.03 eV and 3.26 eV, attributed to the emission of free excitons near the fundamental absorption edge of rutile and anatase, respectively. The influence of TiO<sub>2</sub> crystal structure and calcination temperature of the samples on the PL spectra and optical absorption is discussed.

**Keywords:** Titanium dioxide, Anatase, Rutile, Photoluminescence, Optical absorption.

PACS numbers: 61.46. + w, 61.72.Ji, 71.35. – y, 33.50.Dq

### 1. INTRODUCTION

Titanium dioxide (TiO<sub>2</sub>) belongs to the class of wide-band-gap semiconductors and exists in three polymorphous crystalline modifications: rutile, anatase or brookite. Because of their physical properties (for example, high refraction index and permittivity), as well as high activity in photochemical reactions, TiO<sub>2</sub> is intensively studied during the last decades as a promising material for a wide spectrum of industrial applications, such as solar cells, sensors, microelectronics, catalysis, photocatalysis, electrochemistry, etc.

Anatase is chemically and optically active metastable phase of TiO<sub>2</sub> which is widely used in catalysis and photocatalysis [2]. Rutile is thermodynamically stable polymorphous modification of TiO<sub>2</sub> with high refraction index and coefficient of UV-absorption which is widely used in the production of white pigment [3].

It is known that properties of polydisperse TiO<sub>2</sub> including optical properties significantly depend on the methods of its synthesis, crystal structure, and chemical purity, as well as such characteristics as crystallite size, shape and size of particles, specific area and surface chemistry (defects, density of hydroxyl groups, etc.) [4-7]. On the other hand, optical properties of TiO<sub>2</sub> depend on its electron structure, number and type of defect states (oxygen vacancies) in crystal lattice, since these defect states influence the relaxation processes of photoexcited carriers [1-7]. Influence of these factors on the optical properties of disperse powders of TiO<sub>2</sub> are widely investigated. However, it is often difficult to directly compare the results of different authors in connection with different experimental conditions, sample preparation,

technique and approbation methods. Therefore, titanium dioxide remains the subject of intensive study and discussions.

In the majority of the cases initial conditions of TiO<sub>2</sub> synthesis, parameters of thermal and chemical treatment, crystal structure of the initial compound, particle size and also type and concentration of impurities are the determining factors of discrepancies between the results of different authors. Synthesis method, which allows to obtain samples with controlled crystal phase, size, and morphology of TiO<sub>2</sub> particles, is a very important factor which influences the optical properties of TiO<sub>2</sub>.

Method of photoluminescence spectroscopy is widely used for the investigation of the efficiency of migration, transfer, and capture of charge carriers (electron-hole pairs) in semiconductor oxide materials [5]. It was shown that photoluminescence (PL) spectrum arising as a result of recombination between excited electron-hole pairs strongly depends on the oxide surface state. For example, it is known that surface groups (Ti-OH, Ti-OC<sub>2</sub>H<sub>5</sub>), which form the surface states, effectively suppress PL radiation. These surface states are one of the main factors which influence the exciton radiation [6-9]. Connection between defect concentration and electron relaxation processes in TiO<sub>2</sub> is also important.

As known from the literature, it is almost impossible to observe photoluminescence at room temperature of bulk samples of titanium dioxide, in particular, monocrystals, because of its indirect band nature [10]. At low temperatures one can observe wide bands of anatase PL with the maximum at 2.3 eV with large Stokes shift, which majority of authors ascribed to the recombination of coupled excitons [6, 7]. M. Murakami et al. [9]

\* kern@iop.kiev.ua

have shown that in anatase monocrystal coupled exciton states are stable at temperatures from 5 to 200 K, and above 200 K PL is not observed at all. PL spectra of rutile are studied worse than of anatase.

Excitons in rutile are considered to be “free” [11, 12]. One of the explanations of this fact is that exciton radius in rutile is much larger than the size of elementary cell, therefore, distortion of crystal lattice during exciton nucleation is minimal, and separation of charges or their recombination dominates in the processes of energy transfer. The authors of [13] have shown that for pure anatase position of the PL radiation band is at  $\sim 3.18$  eV, while for pure rutile – at  $\sim 3.02$  eV [14]. It is also established that amorphous structures due to the considerable amount of defect states easy promote the recombination of charges, and, therefore, for such structures PL is not observed.

Haart and Blasse [7] have ascribed a sharp peak at 412 nm (3.01 eV) which is observed in PL spectra of rutile to the radiation of free excitons, and a wide band at 485 nm (2.55 eV) – to the radiation of coupled excitons because of the capture of free excitons by Ti-O groups nearby defects. Amtout [15] has suggested that optical response in the band gap of TiO<sub>2</sub> in the range of 2.7-3.0 eV corresponds to the phonon replicas of 1s exciton. It is known that some TiO<sub>2</sub> samples with nanometer size of TiO<sub>2</sub> particles exhibit photoluminescence at room temperature.

Serpone et al. [16] have considered photoluminescence of colloidal TiO<sub>2</sub> particles with different mean size. It was revealed that levels of traps in anatase are located on the distance of 0.41-0.64 eV from the bottom of the conduction band (CB). Saraf et al. [17] have shown that narrow band in the PL spectrum of polydisperse anatase TiO<sub>2</sub> is resulted from excitons autolocalized at TiO<sub>6</sub> octahedrons. They have also revealed that total intensity of the wide-band PL spectrum increases with the increase in the annealing temperature of samples.

Low-temperature (5-180 K) PL spectra ( $\lambda_{ex} = 260$  nm) of polydisperse TiO<sub>2</sub> (anatase and rutile) were studied in [18]. It was established that in PL spectra of anatase two wide bands with maximums at 2.25 eV and 3.1 eV are observed. With temperature increase from 5 to 140 K intensity of the first band decreases two times, while intensity of the second one decays almost to zero. Rather large Stokes shift of the maximum of PL band relative to the anatase absorption spectrum  $\sim 1.1$ - $1.2$  eV indicates an important role of the electron-phonon relaxation in photoluminescence and is explained by the Franck-Condon principle.

Low-temperature PL spectra of pure rutile at the temperature of 4.2 K ( $\lambda_{ex} = 280$  nm) are also characterized by a wide radiation band with the center at 3.01 eV [18].

The authors of the works [19, 20] have observed the PL of colloidal nanoparticles and nanostructured polydisperse TiO<sub>2</sub> powders at room temperature. Zou et al. [10] have studied ultradisperse TiO<sub>2</sub> particles coated by stearic acid and connected PL at room temperature with the influence of stearic acid on the TiO<sub>2</sub> surface.

In our previous works [21] we have developed the synthesis method of chemically pure single-phase nanocrystalline TiO<sub>2</sub> samples that allowed us to obtain rutile and anatase with close physical and chemical characteristics and investigate their optical properties [22].

In the present work we have performed the comparative investigation of PL at room temperature and optical absorption in the range of 2.7-3.4 eV of pure nanocrystalline polydisperse TiO<sub>2</sub> samples of rutile (*R*) and anatase (*A*) obtained at the same experimental conditions. Connection between the structure, optical absorption and luminescent properties of anatase and rutile are discussed.

## 2. EXPERIMENT

### 2.1 Preparation of the samples

For the investigation we have synthesized polydisperse samples of pure TiO<sub>2</sub> with nanocrystalline structure of rutile (*R*) or anatase (*A*). Samples of rutile (*R1*, *R2*, *R3*, *R4*, and *R5*) were obtained by the thermal hydrolysis of muriatic solutions of TiCl<sub>4</sub> in the presence of colloidal nuclei of rutile [21]. Samples were thoroughly washed and annealed at different temperatures. Crystallite size and specific area were the main peculiarities between synthesized samples of rutile (Table 1).

For synthesis of anatase we have applied two different methods: 1 – thermal hydrolysis of TiCl<sub>4</sub> solution in the presence of colloidal nuclei of anatase at 100 °C (sample *A1*) and 2 – deposition of amorphous titanium hydroxide from TiCl<sub>4</sub> solution by aqueous solution of ammonia (1 : 1) to pH = 6.5 with further thermal hydrolysis at 100 °C (sample *A2*). Initial concentration of muriatic TiCl<sub>4</sub> solutions was 100-110 g/l of TiO<sub>2</sub>; relative molar concentration of TiO<sub>2</sub> / HCl – 3.0-3.2; colloidal fraction of titanium nuclei was equal to 3-5 wt. %. All obtained TiO<sub>2</sub> samples were thoroughly washed by bidistilled water to pH = 6.5 and annealed in air at different temperatures: anatase (*A1*, *A2*) at 300 °C during 12 hours, rutile (*R1*, *R2*) at 300 and 600 °C, respectively, during 12 hours, rutile (*R3*, *R4*, *R5*) at 900 °C during 6 hours (Table 1).

TiO<sub>2</sub> particles consisted of aggregates of nanocrystallites (10-130 nm) and had well crystallized structure of anatase or rutile. Anatase was annealed only at the temperature of 300 °C in order to avoid recrystallization into rutile. Thermal treatment of rutile at 900 °C led to the considerable increase in the nanocrystallite size and decrease in the specific area of the samples to 2-3 m<sup>2</sup>/g (Table 1).

### 2.2 Experimental techniques

Structural properties and phase composition of the synthesized TiO<sub>2</sub> samples were determined by the X-ray diffraction (XRD) method using diffractometer DRON-2 by applying the X-ray radiation CuK<sub>α</sub> ( $\lambda = 1.5406$  Å) and CoK<sub>α</sub> ( $\lambda = 1.7902$  Å). Mean nanocrystallite size of anatase and rutile TiO<sub>2</sub> particles was defined by the broadening of the diffraction maximums of anatase (101) and rutile (110) using the Debye Scherrer formulas

$$D = K\lambda / \beta \cos\theta, \quad (1)$$

where  $D$  is the mean crystallite size in Å;  $K$  is the constant which is equal to 0.89;  $\lambda$  is the wavelength of the X-ray radiation (CuK<sub>α</sub> = 0.15406 nm);  $\beta$  is the total width of the peak on the half of the maximum;  $\theta$  is the diffraction angle.

**Table 1** – Characteristic of TiO<sub>2</sub> samples

Samples	Crystal structure	Annealing temperature °C	Crystal-lite size* nm	O / Ti**	BET m <sup>2</sup> /g
A1	Anatase	300	9**	1.987	137
A2	Anatase	300	10**	1.982	240
R1	Rutile	300	21	1.999	15
R2	Rutile	600	39	2.000	8
R3	Rutile	900	70	2.000	3
R4	Rutile	900	126	2.000	2
R5	Rutile	900	126	2.000	3

\* – XRD analysis, \*\* – RSS analysis

Specific surface of TiO<sub>2</sub> samples was measured by the Brunauer-Emmett-Teller (BET) method. Chemical composition of the samples was determined by the X-ray fluorescence analysis using analyser XNAT-Control.

Raman scattering spectra (RSS) were measured in the spectral region of 80-4000 cm<sup>-1</sup> using spectrometer with Fourier transform Bruker IFS-88 equipped by the add-on FRA-106 at excitation by radiation Nd : YAG of laser ( $\lambda_{ex} = 1.06 \mu$ ) of the power of 300 mW with resolution of 2 cm<sup>-1</sup> at 32 scannings in the geometry of the reverse scattering.

For measurement of the optical absorption spectra in UV and visible range as well as for detection of PL spectra we have used the portable multichannel optical analyzer SL40-2 (3648-pixel CCD-camera with sensor TCD1304AP; diffraction grating 600 g/mm, spectral resolution ~ 0.3 nm; check-in time ~ 7 ms).

Optical absorption spectra of nanocrystalline TiO<sub>2</sub> particles were investigated in the spectral region of 220-750 nm (5.6-1.7 eV) and using radiation of deuterium DDC-30 ( $\lambda_{1max} = 245$  nm and  $\lambda_{2max} = 311$  nm) and xenon DKSH-1000 ( $\lambda_{max} = 472$  nm) lamps as light sources.

To obtain the PL spectra TiO<sub>2</sub> samples were excited by 7-ns pulses of N<sub>2</sub>-laser ( $\lambda_{ex} = 337$  nm) of the power of 50  $\mu$ W with the pulse repetition frequency of 50 Hz. In measurement of PL spectra we have used optical filter for elimination of scattered radiation of N<sub>2</sub>-laser with  $\lambda < 375$  nm. All optical measurements were performed at room temperature. For the investigation of the optical absorption spectra samples were pressed to tablets with KBr with TiO<sub>2</sub> content of ~ 0.1 wt.%.

### 3. RESULTS AND DISCUSSION

#### 3.1 X-ray diffraction analysis and TiO<sub>2</sub> Raman spectra

X-ray diffraction analysis of synthesized samples has shown that all of them have rather good crystal structure and are the pure phase of anatase or rutile (Fig. 1).

Raman scattering spectra of synthesized TiO<sub>2</sub> samples are typical for the crystalline phases of anatase or rutile (Fig. 2a, b) that allows to ascribe the observable bands to the certain types of TiO<sub>2</sub> lattice vibrations [23, 24].

As known, positions of the bands ( $\nu_{max}$ ) of low-frequency vibrations of crystal lattice of the symmetry  $E_g$  (143 cm<sup>-1</sup> for anatase and 447 cm<sup>-1</sup> for rutile) and their half-width ( $\Delta\nu_{1/2}$ ) are very sensitive for the stoichiometric ratio (O / Ti) and TiO<sub>2</sub> crystallite sizes (Fig. 3).

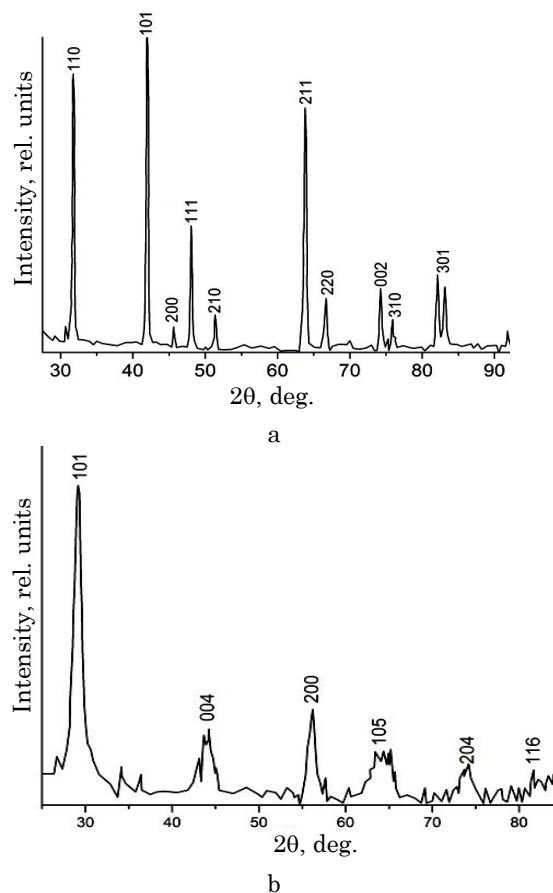


**Fig. 1** – X-ray diffraction spectra of TiO<sub>2</sub> samples at CoK $\alpha$  radiation: rutile – R1 (a) and anatase – A1 (b)

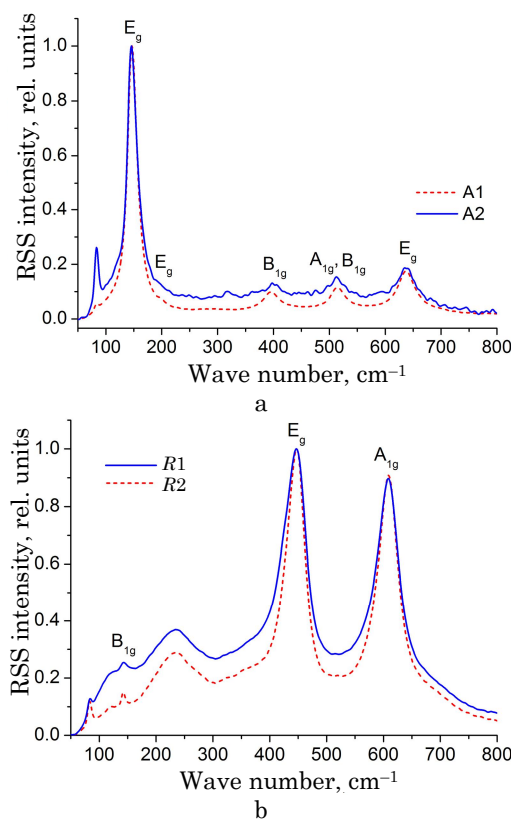


**Fig. 2** – Raman scattering spectra of TiO<sub>2</sub>: a – anatase A1, A2; b – rutile R1, R3

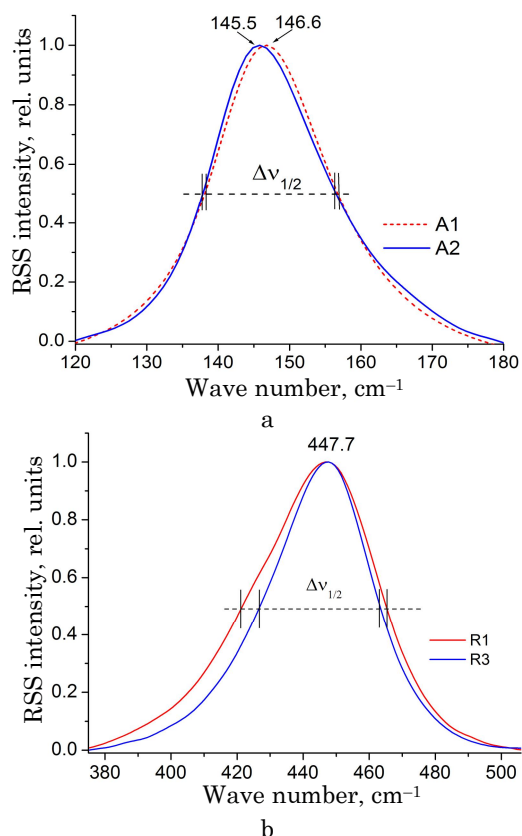


**Fig. 3** –  $E_g$  band in the Raman scattering spectra of anatase A1 and A2 (a) and rutile R1, R3 (b)

On grounds of correlations obtained in [25, 26] and plotted graphs of the dependences of  $\nu_{\max}$  on O / Ti and  $\Delta\nu_{1/2}$  on O / Ti, stoichiometry and sizes of crystallites in the investigated  $\text{TiO}_2$  samples were determined. It was established that stoichiometry of rutile samples higher than of anatase ones, and it is also shown that high-temperature treatment (900 °C) in air atmosphere leads to the increase in the crystallite size and value of correlation O / Ti (Table 1).

### 3.2 $\text{TiO}_2$ optical absorption spectra

Optical absorption of anatase and rutile samples (band gap width is 3.29 and 3.01 eV, respectively [22]) is studied in the spectral region of 2.7-3.6 eV at room temperature (Fig. 4). We have observed some absorption peaks for all  $\text{TiO}_2$  samples nearby the absorption edge (2.8-3.2 eV). Bands with maximums at 2.80, 2.85, 2.91-2.93 and 2.96 eV (Fig. 4, inset) can be connected with the presence of defect states in the band gap of titanium dioxide. Some of these bands were observed earlier [27] at thermal excitation of rutile monocrystals. Khomenko et al. [28] have also observed weak absorption bands on the spectral region between 2.3 and 2.9 eV and ascribed them to the  $d-d$  transitions connected with the localized  $\text{Ti}^{3+}$  states. These weak bands of optical absorption can be also ascribed to the electron transitions from levels connected with oxygen vacancies.

According to [30], absorption peak at 2.91 eV calculated for  $\text{TiO}_2$  corresponds to the lowest energetically allowed indirect transition  $\text{O}2p \rightarrow \text{Ti}3d$  from the valence band (VB) to the conduction band (CB) with participation of phonons. We assume that in our case absorption bands

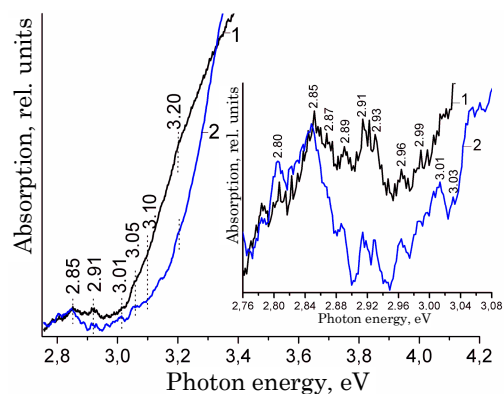


**Fig. 4** – Optical absorption spectra of anatase and rutile  $\text{TiO}_2$  (1 – R1, 2 – A1). On the inset we represent the spectrum fragment in the region of 2.76-3.08 eV

at 2.91-2.93 eV represent superposition of band-to-band fundamental absorption and absorption on defects. The nature of these defect states requires additional investigations.

As seen from Fig. 4, exponential absorption edge of anatase  $\text{TiO}_2$  at  $h\nu > 3.0$  eV is much less sharp than of rutile. Differences in the anatase and rutile spectra in the spectral region of 2.7-3.2 eV is the result of different nature of excitons in these two structures, namely, free excitons in rutile and autolocalized excitons in anatase. At low temperatures such spectra were observed on  $\text{TiO}_2$  monocrystals [32, 33], but as we know for nanocrystalline samples of anatase and rutile at room temperatures we have obtained such data for the first time.

Some features of the optical absorption spectra of nanocrystalline  $\text{TiO}_2$  in the region of intrinsic absorption are denoted by the dotted lines in Fig. 4. In accordance with [30], absorption maximums at 2.91 and 3.05 eV can be ascribed to the allowed indirect transitions from the edge of the Brillouin zone to its center, namely,  $X_{1a}-\Gamma_{1b}$ , and  $X_{2b}-\Gamma_{1b}$ , respectively. Transition on 3.10-3.20 eV can be ascribed to the indirect allowed transition  $\Gamma_3-X_1$  which was observed at 3.11-3.13 eV in the work [34]. Features of the absorption spectrum in the region of energies of  $\sim 3.2$  eV and higher are connected with the beginning of the direct optical transitions to  $\text{TiO}_2$ .

### 3.3 $\text{TiO}_2$ photoluminescence spectra at room temperature

In Fig. 5 we show the PL spectra of nanocrystalline samples of rutile and anatase  $\text{TiO}_2$ . In the spectral region from 2.5 to 3.5 eV a wide radiation band which has clearly expressed thin structure is observed. As we know, such thin structure in the PL spectra of nanocrystalline  $\text{TiO}_2$  was not observed earlier by other authors neither at low nor at room temperatures.

It is known that intensity and structure of the PL spectra depend on the power of excitation source. When using usual commercial fluorimeters, only wide radiation band with maximum at 2.91 eV [7, 16, 35, 19, 36] or wide structureless band [11, 18, 37, 38] was registered in the PL spectra at room temperature. As it was shown in [20], peaks of  $\text{TiO}_2$  radiation with maximums at 2.9 and 2.88 eV were detected when outgoing power of Nd : YAG laser increased to 70 mW.

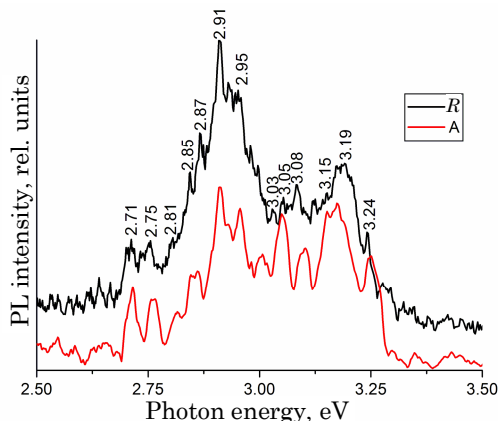


Fig. 5 – PL spectra of TiO<sub>2</sub> rutile R1 (R) and anatase A2 (A)

The authors of [15] for PL excitation in rutile monocrystal have used the tunable dye laser with intensity in a pulse of about  $2,5 \cdot 10^6 \text{ W cm}^{-2}$ . At low temperatures (12-200 K) they have observed the PL spectrum with a thin structure of six peaks. In our case, intensity of N<sub>2</sub>-laser was significantly higher ( $4,4 \times 10^{10} \text{ W cm}^{-2}$  in a pulse) that allowed us to obtain the PL spectra of TiO<sub>2</sub> radiation with thin structure at room temperature.

As seen from Fig. 5, positions of the PL peaks in the radiation spectrum of anatase are almost the same that for rutile, but relative intensities of these peaks are different. We assume that such differences in the PL spectra are connected with different nature of excitons in anatase and rutile which participate in the PL process.

We suggest that PL spectra of nanocrystalline TiO<sub>2</sub> samples in the spectral region of 2.5-3.0 eV (Fig. 5) can be conditioned by the presence of oxygen vacancies and/or defects of crystal lattice. Oxygen vacancies are the intrinsic defects of TiO<sub>2</sub> lattice which generate immediate energy levels in the band gap [39] forming the recombination centers for photoinduced electrons and holes. Positions of the PL peaks with maximums about 2.71, 2.75 and 2.81 eV agree well with the energy levels of traps connected with the presence of oxygen vacancies with two captured electrons (F-centers), [20, 40]. Intensive band with maximum 2.91 eV in the PL spectrum of nanocrystalline anatase and rutile (Fig. 5) can be ascribed to radiation of autolocalized (anatase) or free (rutile) excitons [12], since the same radiation was also observed in the PL spectra of different TiO<sub>2</sub> structures, in particular, monocrystals [7, 11], nanoparticles [17] and colloidal nanoparticles [16]. We have to note that observable in the PL spectrum thin structure of PL bands at 2.71, 2.75 and 2.91 eV require further investigation.

As it is seen from Fig. 5, peak of TiO<sub>2</sub> radiation at 3.03 eV which corresponds to the band gap of rutile [22] is weakly expressed in the obtained PL spectrum. This peak was ascribed to radiation of free excitons [7, 15], and it was not observed earlier at room temperature.

Based on the comparison of the obtained optical absorption and PL spectra of nanocrystalline TiO<sub>2</sub> samples (Fig. 4 and Fig. 5), we can conclude that light absorption and radiation processes nearby the band gap edge occur with participation of the same electron transitions. Photoluminescence of anatase and rutile TiO<sub>2</sub> in high-energy spectral region (with energies higher than the band gap width) can be ascribed to the band-to-band transition from CB to VB.

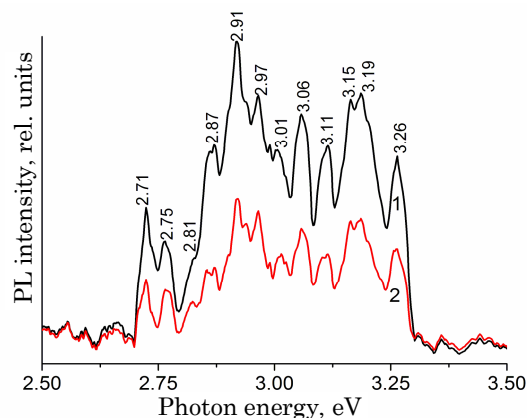


Fig. 6 – PL spectrum of anatase A1 and A2 with different crystallite sizes

According to Daude et al. [30], PL bands at 3.05-3.08 eV and 3.15-3.19 eV can be ascribed to the indirect allowed transitions  $X_2 \rightarrow \Gamma_1$  and  $\Gamma_3 \rightarrow X_1$ , respectively. Peak at 3.24 eV in rutile TiO<sub>2</sub> can be ascribed to the direct allowed transitions  $X_1 \rightarrow X_1$ . Radiation peak at 3.26 eV corresponds to the band gap width in anatase TiO<sub>2</sub> (3.29 eV) [22] and can be ascribed to the emission of free excitons nearby the band gap edge.

In Fig. 6 we show the PL spectra of TiO<sub>2</sub> anatase samples A1 and A2 annealed at 300 °C. Samples were synthesized by two different methods and they differed in the specific surface and stoichiometry (Table 1).

It is seen that in the spectral region of 2.7-3.3 eV radiation intensity of sample A2 is almost two times less than of A1. This fact can be explained by the influence of crystallite size, stoichiometric composition and specific surface of anatase samples on the value of PL intensity. As known, the lesser crystallite size is, the larger content of oxygen vacancies and defects [41, 42] is. Increase in the specific surface is connected with a large amount of surface defect states and high degree of hydration of the samples surface.

In TiO<sub>2</sub> rutile samples behavior of the PL signal considerably differs from that observed for anatase samples. Fig. 7 illustrates the dependence of the PL spectrum of rutile samples R1, R2 and R3 on the annealing temperature. With the increase in the annealing temperature from 300 to 600 °C intensity of PL radiation decreases (R2) and with further temperature rise to 900 °C – it increases (R3). This fact can be connected with both the change in the crystallite size (see Table 1) and different degree of hydration of TiO<sub>2</sub> sample surface. Moreover, change in the PL intensity depending on the annealing temperature of the samples can be connected with the presence of uncontrolled impurities on the surface and inside TiO<sub>2</sub> particles [43, 44] which are desorbed during the sample treatment.

In Fig. 8 we show the PL spectra of rutile samples R3, R4 and R5 annealed at the temperature of 900 °C which have different crystallite size and close values of the specific surface (Table 1). It is seen that PL spectra of these samples are identical.

As shown in the work [45], surface OH-groups and water molecules, connected with two types of the surface active centers (AC), whose binding energy is different, can be present on the TiO<sub>2</sub> surface. Anatase and rutile

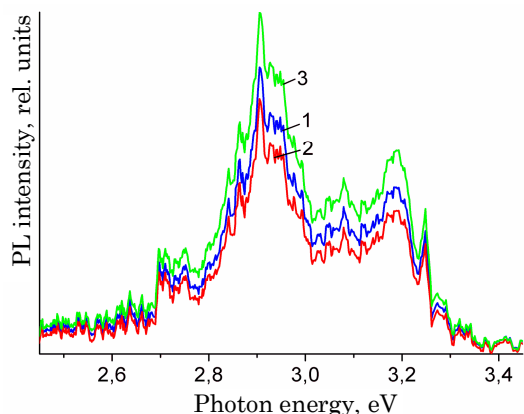


Fig. 7 – PL spectra of rutile: R1 – 300 °C, R2 – 600 °C, and R3 – 900 °C

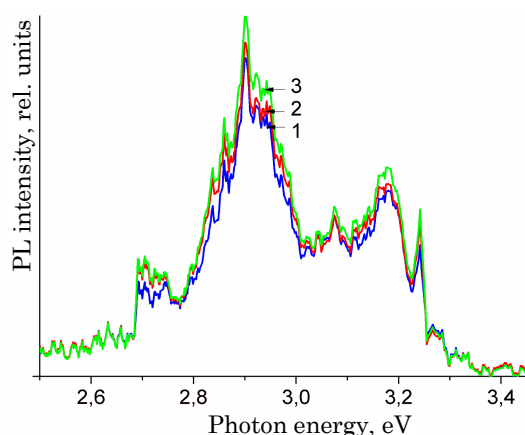


Fig. 8 – PL spectra of rutile: 1 - R3, 2 - R4, and 3 - R5

have similar morphological characteristics but different amount of such surface AC. On the anatase surface annealed at 300 °C there are 70% of “strong” AC with the binding energy of  $\Delta H \sim 7$  kkal/mole and 30% of “weak” AC with  $\Delta H \sim 5$  kkal/mole. On the surface of rutile annealed at 300 °C there are  $\sim 30\%$  of “strong” AC, and because of thermal treatment at 900 °C their amount decreases to 7%.

Photoinduced holes can be easily trapped by the chemisorbed surface hydroxyl groups with the formation of  $\bullet\text{OH}$  hydroxyl radicals. Effects of the PL quenching by

hydroxyls were detected for the rare-earth ions [46] and aqueous suspensions of nanoparticles [47]. At thermal treatment (300-900 °C) degree of hydration of the surface of  $\text{TiO}_2$  samples (a number of the surface hydroxyl groups) significantly decreases. This leads to the decrease in the effectiveness of PL quenching, i.e. increase in its intensity in the radiation spectrum of rutile.

#### 4. CONCLUSIONS

Investigation of the optical absorption in the range of 2.7-3.6 eV and photoluminescence of nanocrystalline  $\text{TiO}_2$  samples of anatase and rutile at room temperature has been performed in the work. Bands of the exciton and band-to-band luminescence at room temperature have been registered for the first time during excitation of  $\text{TiO}_2$  by the pulsed nitrogen laser. It is established that light absorption and radiation processes nearby the band gap edge occur with the participation of the same electron transitions. In PL spectra of anatase and rutile  $\text{TiO}_2$  radiation bands in the range of 2.71-2.81 eV appear as a result of exciton  $e^-h^+$  recombination through oxygen vacancies. Intensive band of the exciton PL at 2.91 eV is conditioned by the recombination of autolocalized excitons in anatase and free excitons in rutile. PL bands with maximums 3.03 eV in rutile and 3.26 eV in anatase correspond to the edge annihilation of free excitons. PL bands in the range of 3.0-3.3 eV belong to direct and indirect transitions in anatase and rutile  $\text{TiO}_2$ .

It is shown that increase in the nanocrystallite size with the increase in the temperature of thermal treatment does not lead to the appreciable change in the PL spectra of rutile. This can be conditioned by the competition of two effects: decrease in the PL intensity because of the decrease in the number of defect states and decrease in the effectiveness of PL quenching by surface OH-groups. Intensity of the exciton PL of  $\text{TiO}_2$  anatase samples decreases with the increase in the specific surface that can be connected with luminescence quenching due to the increase in the amount of surface OH-groups.

#### ACKNOWLEDGEMENTS

This work has been performed under the financial support of the National Academy of Sciences of Ukraine within the framework of the grant program “Nanophysics and nanoelectronics” (project No VTs-157).

#### REFERENCES

1. M Diebolt, *Surf. Sci. Rep.* **48**, 53 (2003).
2. A. Fujishima, X. Zhang, D.A. Tryk, *Surf. Sci. Rep.* **63**, 515 (2008).
3. M. Anpo, Y. Kubokawa, *Rev. Chem. Intermed.* **8**, 105 (1987).
4. M.A. Henderson, *Surf. Sci. Rep.* **66**, 185 (2011).
5. T. Sekiya, S. Kamei, S. Kurita, *J. Lumin.* **87-89**, 1140 (2000).
6. Y.C. Zhu, *J. Solid State Chem.* **145**, 711 (1999).
7. L.G.J. De Haart, G. Blasse, *J. Solid State Chem.* **61**, 135 (1986).
8. H. Tang, K. Prasad, R. Sanjines, P.E. Schmid, F. Levy, *J. Appl. Phys.* **75**, 2042 (1994).
9. M. Murakami, Y. Matsumoto, K. Nakajima, T. Makino, Y. Segawa, T. Chikyow, P. Ahmet, M. Kawasaki, H. Koinuma, *Appl. Phys. Lett.* **78**, 2664 (2001).
10. B. Zou, L. Xiao, T. Li, J. Zhao, Z. Lai, S. Gu, *Appl. Phys. Lett.* **59**, 1826 (1991).
11. H. Tang, H. Berger, P.E. Schmid, F. Levy, *Solid-State Comm.* **92**, 267 (1994).
12. H. Tang, F. LeBy, H. Berger, P.E. Schmid, *J. Phys. Rev. B* **52**, 7771 (1995).
13. H. Tang, K. Prasad, R. Sanjines, P.E. Schmid, F. L'evy, *J. Appl. Phys.* **75**, 2024 (1994).
14. J.H. Jho, *J. Alloy. Compd.* **459**, 386 (2008).
15. A. Amtout, R. Leonelli, *Phys. Rev. B* **51**, 6842 (1994).
16. N. Serpone, D. Lawless, R. Khairutdinov, *J. Phys. Chem.* **99**, 16646 (1995).
17. L.V. Saraf, S.I. Patil and S.B. Ogale, *J. Mod. Phys. B* **12**, 2635 (1998).
18. V. Melnyk, V. Shymanovska, G. Puchkovska, T. Bezrodna, G. KlisheBich, *J. Mol. Str.* **744-747**, 573 (2005).
19. Y. Zhu, C. Ding, G. Ma, Z. Du, *J. Solid State Chem.* **139**, 124 (1998).

20. N.D. Abazovic, M.I. Comor, M.D. Dramicanin, D.J. Jovanovic, S.P. Ahrenkiel, and J.M. Nedeljkovic, *J. Phys. Chem. B* **110**, 25366 (2006).
21. V.V. Shimanovskaya, A.A. Dvernyakova, V.V. Strelko, *Izv. AN SSSR, Neorg. Mater.* **24**, 1188 (1988).
22. L. Kernazhitsky, V. Shymanovska, T. Gavrilko, V. Naumov, V. Kshnyakin, T. Khalyavka, *J. Solid State Chem.* **198**, 511 (2013).
23. P.S. Narayanan, *Proc. Indian Acad. Sci. Sect. A* **32**, 279 (1950).
24. S.P.S. Porto, P.A. Fleury, T.C. Damen, *Phys. Rev.* **154**, 522 (1967).
25. J.C. Parker, R.W. Siegel, *Appl. Phys. Lett.* **57**, 943 (1990).
26. W.F. Zhang, Y.L. He, M.S. Zhang, Z. Yin, Q. Chen, *J. Phys. D: Appl. Phys.* **33**, 912 (2000).
27. A.K. Ghosh, F.G. Wakim, R.R. Addiss, Jr., *Phys. Rev.* **184**, 979 (1969).
28. V.M. Khomenko, K. Langer, H. Rager, A. Fett, *Phys. Chem. Miner.* **25**, 338 (1998).
29. M. Watanabe, T. Hayashi, H. Yagasaki, S. Sasaki, *Intern. J. Mod. Phys. B* **15**, 3997 (2001).
30. N. Daude, C. Gout, and C. Jouanin, *Phys. Rev. B* **15**, 3229 (1977).
31. L. Jing, B. Xin, F. Yuan, L. Xue, B. Wang, H. Fu, *J. Phys. Chem. B* **110**, 17860 (2006).
32. H. Tang, H. Berger, P.E. Schmid, F. Levy, *Solid-State Commun.* **92**, 267 (1994).
33. M. Watanabe, S. Sasaki, T. Hayashi, *J. Lumin.* **87-89**, 1234 (2000).
34. K. Vos, H.J. Krusemeyer, *Solid-State Commun.* **15**, 949 (1975).
35. M. Anpo, N. Aikawa, Y. Kubokawa, M. Che, C. Louis, E. Giamello, *J. Phys. Chem.* **89**, 5017 (1985).
36. F. Dong, W. Zhao, Z. Wu, S. Guo, *J. Hazard. Mater.* **162**, 763 (2009).
37. T. Sekiya, M. Igarashi, S. Kurita, S. Takekawa, M. Fujisawa, *J. Electron. Spectrosc.* **92**, 247 (1998).
38. K. V. Baiju, A. Zachariah, S. Shukla, S. Biju, M.L.P. Reddy, K.G.K. Warriar, *Catal Lett.* **130**, 130 (2009).
39. M. Gratzel, *Heterogeneous Photochemical Electron Transfer* (XRC Press, Inc.: 1989).
40. Y. Lei, D. Zhang, G.W. Meng, G.H. Li, X.Y. Zhang, C.H. Liang, W. Chen, S.X. Wang, *Appl. Phys. Lett.* **78**, 1125 (2001).
41. D.Z. Li, Y. Zheng, X.Z. Fu, *Chin. J. Mater. Res.* **14**, 639 (2000).
42. L.D. Zhang, J.M. Mou, *Nanomaterials and Nanostructure* (Science Press: Beijing: 2001).
43. J.A. Nelson, E.L. Brant, M.J. Wagner, *Chem. Mater.* **15**, 688 (2003).
44. T. Bezrodna G. Puchkovska, V. Shymanovska, J. Baran, H. Ratajcz, *J. Mol. Struct.* **700**, 175 (2004).
45. T. Bezrodna, G. Puchkovska, V. Shymanovska, I. Chashecnikova, T. Khalyavka, J. Baran, *Appl. Surf. Sci.* **214**, 222 (2003).
46. W.D. Horrocks Jr., D.R. Sudnick, *Acc. Chem. Res.* **14**, 384 (1981).
47. R. Schmechel, M. Kennedy, H. von Seggern, H. Winkler, M. Kolbe, R.A. Fischer, L. Xiaomao, A. Benker, M. Winterer, H. Hahn, *J. Appl. Phys.* **89**, 1679 (2001).